

# Threshold characteristics analysis of InP-based PhC VCSEL with buried tunnel junction

Saeid Marjani\* and Seyed Ebrahim Hosseini

Department of Electrical Engineering  
Ferdowsi University of Mashhad  
Mashhad, Iran  
[\\*saeid.marjani@stu-mail.um.ac.ir](mailto:saeid.marjani@stu-mail.um.ac.ir)  
[ehosseini@um.ac.ir](mailto:ehosseini@um.ac.ir)

Rahim Faez

Department of Electrical Engineering  
Sharif University of Technology  
Tehran, Iran  
[faez@sharif.ac.ir](mailto:faez@sharif.ac.ir)

**Abstract**— The comprehensive optical-electrical-gain-thermal self-consistent model of the 1.55  $\mu\text{m}$  AlGaInAs Photonic Crystal vertical cavity surface emitting diode lasers (PhC VCSELs) with buried tunnel junction (BTJ) has been applied to optimize its threshold characteristics. It shows that, for 5  $\mu\text{m}$  devices, the room temperature (RT) threshold current equal to only 0.59 mA and maximum operating temperature equal to as much as 380 K. Results suggest that, the 5  $\mu\text{m}$  AlGaInAs PhC VCSELs seem to be the most optimal ones for light sources in high performance optical communication systems.

## I. INTRODUCTION

The Vertical cavity surface emitting diode lasers (VCSELs) are very attractive light sources used in high performance optical communication systems and tunable diode laser spectroscopy, since they offer: single longitudinal mode operation, low threshold current, high-output power, high speed modulation, a circular beam profile and low manufacture cost [1], [2]. The first continuous wave (CW) lasing operation of long wavelength InP-based VCSELs was indicated in 1979 by Soda et al. [3] but their technology has not been improved drastically within these years. That means that there are still several issues necessary to improve the reliability of InP-based VCSELs. To name the most important issues we have to mention not a good combination of materials for distributed Bragg reflectors (DBRs) requirements for lattice matching to InP, large index difference and high thermal conductivity [4], too high free carrier absorption in p-type layers in the InP-based long wavelength, especially for 1.55  $\mu\text{m}$  [5], lack of the confinement of both current spreading and optical fields and high temperature of device operation.

Recently, some of the solutions have been found to the issues mentioned in order to improve 1.55  $\mu\text{m}$  InP-based VCSELs structures [6]-[10]. First, the material systems discussed for 1.55  $\mu\text{m}$  InP-based lattice-matched DBRs include AlGaInAs/AlInAs [6], air gap/InP DBR [7] and the more recently investigated AlGaInAs/InP [8] that is most attractive due to easier growth by MOCVD. Second, it is necessary to using a buried tunnel junction in order to funnel

the injection current into a spot with the small diameter in the center of the active region [9]. In this way, the total optical absorption becomes small and the injection current of VCSELs becomes much more uniform laterally when current injection through n-type layer and tunnel junction. Of course, it can confine current and light to any size and shape. And finally, it is necessary to using the photonic crystals (PhC) in order to assure single mode operation for broader current apertures [10]. It is very attractive, since it offers: ability to select very narrow spectrum of allowed frequencies [11] and discriminate all higher-order modes.

The optimized structure is the structure that has the lower lasing thresholds and the higher lasing operation temperature. Consequently, the main goal of this work is to optimize 1.55  $\mu\text{m}$  PhC VCSEL with AlGaInAs/InP DBRs and BTJ on InP substrates in order to propose a VCSEL structure which simultaneously reveals the low lasing threshold at room temperature.

## II. THE MODEL

The comprehensive optical-electrical-gain-thermal self-consistent model used here to simulate the InP-based PhC VCSELs Composed of four interrelated parts: The scalar optical approach is based on effective frequency method (EFM) [12], the finite element (FE) electrical and thermal models [13], and the gain model is based on the Fermi's golden rule [14].

In addition, all important, usually non-linear, interactions between the optical, electrical, thermal and recombination phenomena are also taken into account with the aid of the self-consistent iteration algorithm, including [13]: gain-induced wave-guiding, thermal focusing, self-focusing, temperature dependence of optical gain and absorption coefficients and the energy gaps and electrical conductivities and thermal conductivities, carrier-concentration dependence of electrical conductivities and optical gain and absorption coefficients and the energy gaps and wavelength dependences of optical gain and absorption coefficients.

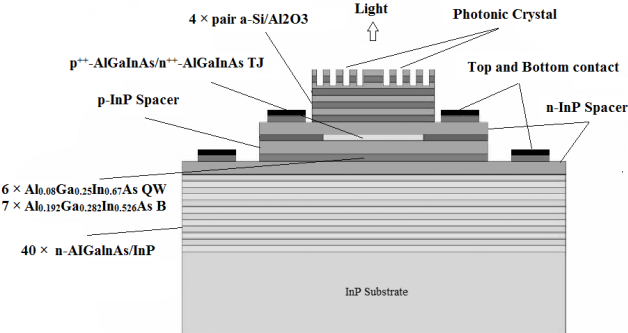


Figure 1. Schematic structure of the  $1.55\text{ }\mu\text{m}$  BTJ-VCSEL device.

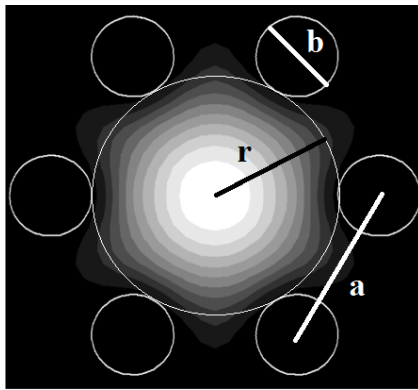


Figure 2. Intensity distribution of the fundamental mode within the active region and the first ring of the photonic crystal. The diameter of the PhC holes ( $b$ ), the distance between the holes ( $a$ ) and the optical aperture ( $2r$ ) are defined.

Consequently, several factors are effective in determining the profiles of all model parameters within the whole VCSEL volume, including: different chemical compositions of the VCSEL layers, the distributions of the temperature, the current density, the carrier concentration and the mode radiation intensity. Heat loss from the modeled PhC VCSELs device was specified using thermal contacts at the top electrode, bottom electrode and the device sidewall. The thermal contacts define thermal conductivities to simulate heat loss from radiation via exposed surfaces or conduction through the semiconducting material to a heat-sink.

### III. THE STRUCTURE

The structure investigated here is the  $1.55\text{ }\mu\text{m}$  PhC VCSEL incorporating an AlGaInAs/InP active cavity, AlGaInAs/InP DBRs and BTJ that it has been developed based on the experimental device which has been reported in [8]. As shown in Fig. 1, it is composed of six  $\text{Al}_{0.08}\text{Ga}_{0.25}\text{In}_{0.67}\text{As}$  wells with 1% compressive strain and seven  $\text{Al}_{0.192}\text{Ga}_{0.282}\text{In}_{0.526}\text{As}$  barriers within a cavity terminated on both sides by DBRs: a 4-pair a-Si/Al<sub>2</sub>O<sub>3</sub> p-type DBR and a 40-pair n-AlGaInAs/InP n-type DBR. The maximum reflectivity is 99.4% and 99.9% for p-type and n-type DBR, respectively. Above the active layers and GaInAsP etch stop layer, tunnel junction composed of a p<sup>+</sup>-AlGaInAs/n<sup>+</sup>-AlGaInAs is located. The tunnel junction is thin, and its layer's bandgap is wider than the bandgap of the quantum wells to avoid optical absorption.

Following the procedure originally outlined by Nishiyama et al. in [8], the triangular-lattice air holes in the p-type DBR is designed for single-mode operation for this VCSEL structure. The optical confinement is achieved by means of three rings of the hexagonal air-hole PhC where the center is missed off to make the defect region. The photonic crystal is determined accordingly to the PhC pitch ( $a$ ), hole diameter ( $b$ ), depth of the PhC holes ( $d$ ) and optical aperture ( $2r=2a-b$ ) as have been defined in Fig. 2. The optical aperture is defined as a circle of radius  $r$  that touching the inner ring of PhC holes. The structure under consideration is defined by  $r=2\text{ }\mu\text{m}$ ,  $d=8\text{ }\mu\text{m}$  and  $b/a = 0.5$ , which have been chosen to assure high modal gain [15].

### IV. THE RESULTS

Change in the ambient temperature causes important changes of values of material parameters. On one hand, increase in the ambient temperature causes a decrease in the energy gaps, electrical and thermal conductivity values, but the other hand, causes an increase in the refractive indices, optical absorption coefficients and Auger recombination efficiency. Consequently, VCSEL performance is fundamentally decreased by changing the important physical phenomena such as current spreading, optical field confinement and radiation absorption. Hence, with the gradual increase in ambient temperature, threshold current is increased and quantum efficiency is reduced because of the reduction of the peak gain with increasing temperature.

Fig. 3 shows the dependence of the threshold gain as a function of tunnel junction diameter at room temperature. As one can see, by increasing of tunnel junction size causes a decrease in threshold gain and an increase in wavelength, mainly because of better radial confinement of the fundamental mode. The structure supports only the fundamental mode for narrow tunnel junction diameters lower than  $6\text{ }\mu\text{m}$ . Further increase of the diameter of the tunnel junction support higher order modes, and it causes worse overlapping of an optical gain and the intensity profile of the fundamental mode.

The threshold current as a function of the tunnel junction diameter at room temperature is plotted Fig. 4. As shown, when the tunnel junction diameter increases, the threshold current shows the same rule as that at the threshold gain which should be mainly due to provide favorable carrier concentration in the active region. The lowest threshold current is  $0.48\text{ mA}$  for  $5\text{ }\mu\text{m}$  device.

The analysis of the maximum ambient temperature as a function of the tunnel junction diameter is given in the Fig. 5. As one can see, the increase in the tunnel junction diameter is initially followed by a rather insignificant decrease in the maximum ambient temperature but, for large tunnel junctions, this decrease becomes much more considerable.

The analysis of the optical wavelength as a function of the tunnel junction diameter is given in the Fig. 6. As can be seen, an increase in the tunnel junction diameter is followed by a better radial confinement of the fundamental mode which causes an increase in optical wavelength. For tunnel junction diameters exceeding  $6\text{ }\mu\text{m}$ , optical wavelength is reduced due

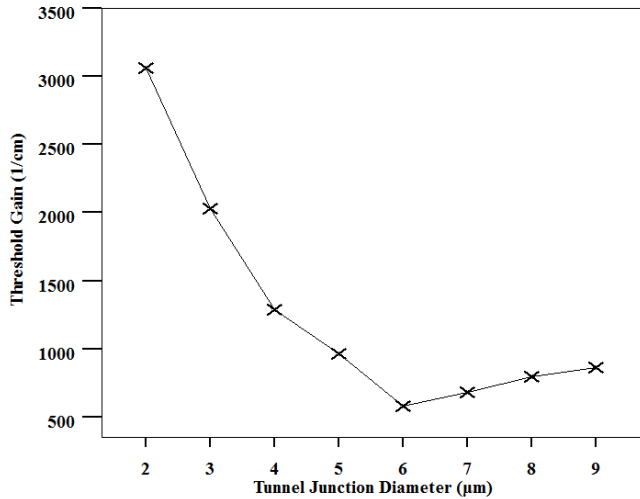


Figure 3. Threshold gain as a function of the tunnel junction diameter at room temperature.

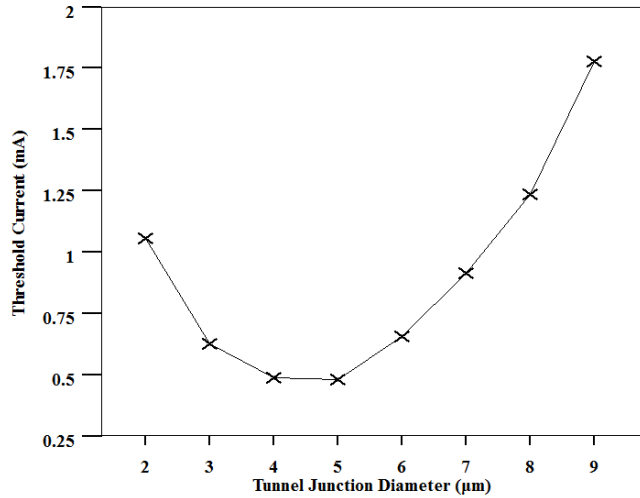


Figure 4. Threshold current as a function of the tunnel junction diameter at room temperature.

to Increasing the active region gain non-uniformity leads to worse overlap between gain and the fundamental mode intensity profile.

On the one hand, the threshold current is as low as 0.75 mA for TJ diameters from 3 to 6  $\mu\text{m}$  and on the other hand, the maximal ambient temperature is as high as 350–380 K for TJ diameters from 2 to 6  $\mu\text{m}$ . The optimized structure is the structure that has the lower lasing thresholds and the higher lasing operation temperature. Therefore, it seems that the most optimal tunnel junction diameter for modeled VCSEL structure should have 5  $\mu\text{m}$ , which enables both lowest threshold current and highest operating temperature. For modeled VCSEL structure, threshold current and maximal ambient temperature are 0.48 mA and 360 K, respectively.

## V. CONCLUSION

The AlGaInAs multi quantum well (MQW) Photonic Crystal vertical cavity surface emitting diode lasers (PhC

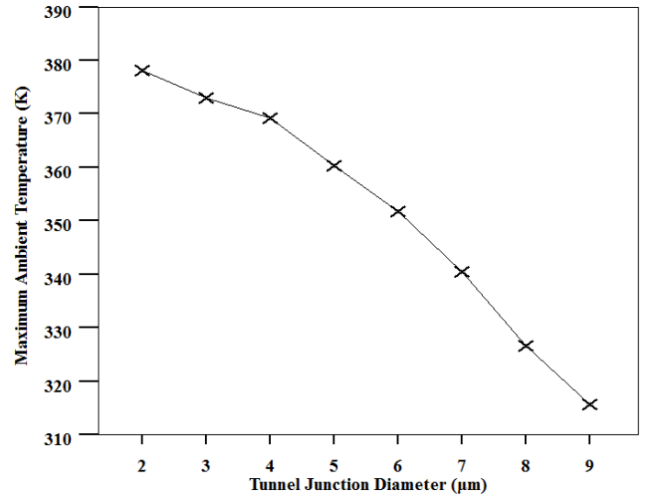


Figure 5. Maximum ambient temperature versus the tunnel junction diameter.

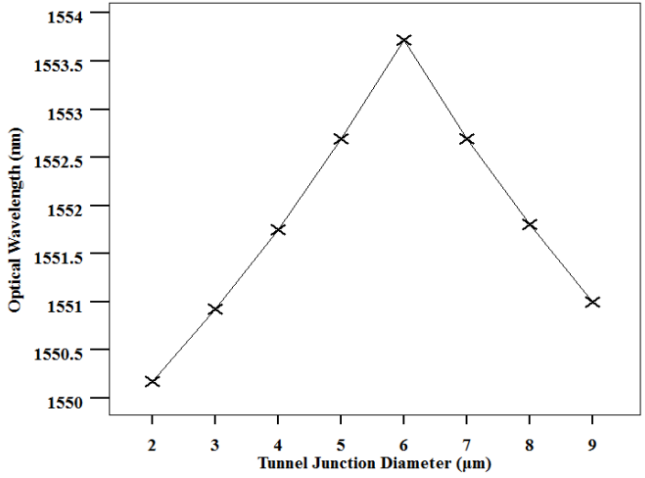


Figure 6. Optical wavelength versus the tunnel junction diameter at room temperature.

VCSELs) with buried tunnel junction (BTJ) with sub-mA threshold current for a wide range of TJ diameter have been investigated. Although the devices show lasing up to about 380 K, a well-defined diameter of the tunnel junction should lead to improved temperature characteristics. We conclude that the most optimal diameter should have 5  $\mu\text{m}$  because it shows both the lowest threshold current and the highest operating temperature.

## REFERENCES

- [1] S.-Y. Hu, J. Ko, and L. A. Coldren, "High-performance densely packed vertical-cavity photonic integrated emitter arrays for direct-coupled WDM applications," *IEEE J. Photon. Technol. Lett.*, vol. 10, pp. 766–768, June 1998.
- [2] K. Iga, "Surface-emitting laser—Its birth and generation of new optoelectronics field," *J. Sel. Topics Quantum Electron.*, vol. 6, pp. 1201–1215, Nov./Dec. 2000.

- [3] H. Soda, K. Iga, C. Kitahara, and Y. Suematsu, "GaInAsP/InP surface emitting injection lasers," *Jpn. J. Appl. Phys.*, vol. 18, pp. 2329–2330, 1979.
- [4] A. Karim, J. Piprek, P. Abraham, D. Lofgreen, Y. J. Chiu, and J. E. Bowers, "1.55  $\mu\text{m}$  vertical-cavity laser arrays for wavelength division multiplexing," *J. Sel. Topics Quantum Electron.*, vol. 7, pp. 178–183, Mar./Apr. 2001.
- [5] N. Nishiyama, C. Caneau, B. Hall, G. Guryanov, M.H. Hu, X.S. Liu, M.J. Li, R. Bhat, and C.E. Zah, "Long-Wavelength Vertical-Cavity Surface-Emitting Lasers on InP With Lattice Matched AlGaInAs-InP DBR Grown by MOCVD," *IEEE J. Sel. Top. Quant.*, vol.11, pp. 990-998, Sept.-Oct. 2005.
- [6] R. Shau, M. Ortsiefer, J. Rosskopf, G. Böhme, C. Lauer, M. Maute, and M.-C. Amann, "Long-wavelength InP-based VCSELs with Buried tunnel junction: Properties and applications," in Proc. 2004 SPIE, pp. 1–15.
- [7] S. Boutami, B. Ben Bakir, P. Regreny, J.L. Leclercq and P. Viktorovitch, "Compact 1.55  $\mu\text{m}$  room-temperature optically pumped VCSEL using photonic crystal mirror," *IEEE J. Electron. Lett.*, vol. 43, pp. 37-38, March 2007.
- [8] N. Nishiyama, "InP-based VCSELs with AlGaInAs/InP DBR and their applications," in Proc. 2008 Conf. International Nano-Optoelectronics Workshop, pp. 46-48.
- [9] E. Kapon, A. Sirbu "Long-wavelength VCSELS Power efficient answer," *J. Nat. Photon.*, vol. 3, pp. 27-28, 2009
- [10] D. F. Siriani, M. P. Tan, A. M. Kasten, A. C. Lehman Harren, P. O. Leisher, J. D. Sulkin, J. J. Raftery, Jr., A. J. Danner, A. V. Giannopoulos, K. D. Choquette "Mode Control in Photonic Crystal Vertical-Cavity Surface-Emitting Lasers and Coherent Arrays," *IEEE J. Sel. Top. Quantum Electron.*, vol. 15 pp. 909-917, May-june 2009.
- [11] R. De La Rue "Photonic Crystal Components: Harnessing the Power of the Photon," *J. Optics and Photonics News*, vol. 17, pp. 30-35, 2006.
- [12] H. Wenzel and H.J. Wünsche, "The effective frequency method in the analysis of vertical-cavity surface-emitting lasers," *IEEE J. Quantum Elect.*, vol.33, pp. 1156–1162, Jul. 1997.
- [13] R.P. Sarzala and W. Nakwaski, "Optimisation of the 1.3- $\mu\text{m}$  GaAs-based oxide-confined (GaIn)(NAs) vertical-cavity surface-emitting lasers for their low-threshold room-temperature operation," *J. Phys. Condens. Mat.*, vol.16, pp. S3121–S3140, 2004.
- [14] R.P. Sarzala, "Designing strategy to enhance mode selectivity of higher-output oxide-confined verticalcavity surface-emitting lasers," *J. Appl. Phys. A*, vol. 81, pp. 275-283, Jul. 2005.
- [15] T Czyszanowski, M. Dems, K. Panajotov "Optimal parameters of Photonic-Crystal Vertical-Cavity Surface-Emitting Diode Lasers," *IEEE J. Light. Technol.*, vol. 25, pp. 2331 – 2336, Sept. 2007.